catalysts

MDPI

Article

Highly Efficient Heterogeneous Pd@POPs Catalyst for the N-Formylation of Amine and CO_2

Guoqing Wang [1,2], Miao Jiang [1], Guangjun Ji [1,2], Zhao Sun [1,2], Lei Ma [1], Cunyao Li [1], Hong Du [1], Li Yan [1,2,*] and Yunjie Ding [1,2,3,*]

[1] Dalian National Laboratory for Clean Energy, Dalian Institute of Chemical Physics, Chinese Academy of Sciences, Dalian 116023, China; wangguo17@dicp.ac.cn (G.W.); jiangmiao87@dicp.ac.cn (M.J.); jgj198815@dicp.ac.cn (G.J.); sunzhao@dicp.ac.cn (Z.S.); mlburning@dicp.ac.cn (L.M.); licunyao2008@dicp.ac.cn (C.L.); duhong200@dicp.ac.cn (H.D.)
[2] University of Chinese Academy of Sciences, Beijing 100049, China
[3] State Key Laboratory of Catalysis, Dalian Institute of Chemical Physics, Chinese Academy of Sciences, Dalian 116023, China
* Correspondence: yanli@dicp.ac.cn (L.Y.); dyj@dicp.ac.cn (Y.D.); Fax: +86-411-8437-9143 (L.Y. & Y.D.)

Abstract: Utilization of CO_2 for the production of fine chemicals has become a research hotspot for a long time. In order to make use of CO_2, we developed a highly efficient heterogeneous catalyst (denoted as Pd@POPs) for the N-formylation reaction of amine and CO_2 under mild conditions. The Pd catalyst was based on a porous organic polymer derived from the solvothermal polymerization of vinyl-functionalized PPh_3. A series of characterizations and comparative experiments demonstrated that the Pd@POPs catalyst has high BET (Brunauer-Emmett-Teller) surface areas, hierarchical pore structure, and uniform dispersion of Pd active sites resulting from the formation of strong coordination bonds between Pd species and P atoms in the porous organic polymer (POP) support. In addition to the excellent activity, the Pd@POPs catalyst shows good stability for the N-formylation reaction of amine and CO_2.

Keywords: N-formylation; carbon dioxide; heterogeneous catalyst; porous organic polymer

Citation: Wang, G.; Jiang, M.; Ji, G.; Sun, Z.; Ma, L.; Li, C.; Du, H.; Yan, L.; Ding, Y. Highly Efficient Heterogeneous Pd@POPs Catalyst for the N-Formylation of Amine and CO_2. *Catalysts* **2021**, *11*, 220. https://doi.org/10.3390/catal11020220

Academic Editor: Leonarda Francesca Liotta
Received: 11 January 2021
Accepted: 2 February 2021
Published: 7 February 2021

1. Introduction

Carbon dioxide (CO_2) is an abundant, low-cost, sustainable, and nontoxic C1 raw material. The transformation of CO_2 into value-added chemicals has attracted wide attention in academia and the industry. Additionally, the utilization of CO_2 as a carbon source for fine chemical synthesis can contribute to the reduction of CO_2 in the atmosphere [1–3]. Great efforts have been made by researchers for the conversion of CO_2 into value-added chemicals, such as formic acid [4,5], cyclic carbonates [6–8], and formamides [9]. Formamides are often used as intermediates for the synthesis of fine chemicals [10,11], Vilsmeier–Haack reaction, and solvents [12,13], and their production is one of the potential ways for the fixation of CO_2. For example, N,N-dimethylformamide (DMF) is produced by an NaOOCH-catalyzed reaction of dimethylamine with CO in industrial production [14]. However, the toxic CO hampers its wider use. The carbonylation reaction using cheap and abundant CO_2 is a safer way to synthesize organic chemicals. Using CO_2 as C1 block and H_2 as formylating reductant is a substitute green way for the N-formylation of amines.

In recent years, various homogeneous catalysts have been developed to improve the efficiency of N-formylation reaction under mild conditions. The most active homogeneous catalyst with a TON (Turnover Number) of up to 1,940,000 for the N-formylation of morpholine was developed by Ding [15], which is a pincer catalyst based on Ru coordinated with P and N atoms in the form of tridentate chelating ligand. Milstein et al. reported another similar chelating coordination catalyst based on Co, and a yield of up to 99% was achieved within 36 h at 150 °C, $P_{CO2} = P_{H2} = 30$ bar [16]. Homogeneous catalysts

possess highly catalytic activity due to their well-defined and uniform single active sites. Nevertheless, homogeneous catalysts suffer the problem of catalyst recyclability. Thus, heterogeneous catalysts are desirable for industrial applications because they allow easy separations and catalyst recovery and recycle. A large number of heterogeneous catalysts supported on inorganic materials (including PAL [17], TiO_2 [18], and so on [19]) have been developed for N-formylation reaction. For instance, Kaneda et al. reported that the Au-based TiO_2 catalyst exhibited excellent activity and reusability for the catalysis of the selective N-formylation of functionalized amines [18]. Recently, few metal catalysts immobilized on porous organic polymers (POPs) have been explored for N-formylation reaction. Compared with conventional inorganic supports, POPs stand out for their permanent porosity, high surface areas, good thermal stability, and structure diversity [20]. For example, Liu et al. synthesized pyridine-functionalized porous organic polymers (CarPy-CMP) and CarPy-CMP@Ru. Morpholine in this catalytic system can get a conversion of 97% and a yield of 94% at $P_{CO2} = P_{H2} = 4$ MPa at 130 °C within 24 h [21].

Our group has been committed to the preparation and application of triphenylphosphine-based porous organic polymers. Rh/POL-PPh_3 [22], Rh/CPOL-BP&PPh_3 [23], and Rh/CPOL-BP&$P(OPh)_3$ [24] have been applied in the hydroformylation of ethylene, propylene, and butene, respectively. These catalysts exhibited exciting catalytic activity and stability. We have also designed and synthesized another two kinds of highly active catalysts (PPh_3-ILX@POPs [8] and Mg-por/pho@POPs [25] for CO_2 conversion). From our previous research, we know that the phosphine-rich backbone has a strong adsorption capacity for CO_2 and can fix metals, thus preventing metal loss [8]. Inspired by that, we envisioned a promising application of heterogeneous Pd@POPs as catalysts for the N-formylation of amine and CO_2. Here, in order to expand the application of POP materials easily obtained in nearly 100% yield, a general and highly efficient Pd-based heterogeneous catalyst synthesized by the solvothermal polymerization of 3v-PPh_3 for N-formylation reaction was developed. A conversion of 93% was obtained under mild conditions, such as 100 °C, $P_{CO2} = P_{H2} = 3$ MPa, within 24 h. Besides its excellent performance, the Pd@POPs catalyst is more applicable to secondary amines than primary amines and more stable than other common Pd catalysts supported on an inorganic carrier due to the formation of Pd–P coordination bonds.

2. Results and Discussions

The synthesis method of the Pd@POPs catalyst is illustrated in Scheme 1. The vinyl-functionalized PPh_3 ligand was polymerized under solvothermal conditions (THF, 100 °C); then $Pd(OAc)_2$ was added to the reaction mixture.

The pore structure of the catalyst can be determined from the N_2 adsorption–desorption isotherm (Figure 1a) and pore size distribution (Figure 1b). The Pd@POPs exhibits high BET surface areas and pore volume (900.3 m^2/g and 1.504 cm^3/g). The pore size distribution is calculated by the nonlocal density functional theory (NLDFT) method. The pore sizes of Pd@POPs are mainly distributed in the region of micropores (<2 nm) and mesopores (2–10 nm). The existence of micropores can be determined by the region of $P/P_0 = 0$–0.01. The hysteresis loop in the N_2 adsorption–desorption isotherm suggests the existence of mesopores. The TEM image (Figure 1c) and SEM image (Figure 1d) for Pd@POPs also provide evidence for the hierarchical porosity that facilitates the diffusion of reactants and products during the reaction. Furthermore, the good thermal stability of POP and Pd@POPs is proved by thermal gravimetric analysis (TGA, Figure S1). The initial decomposition temperature is 400 °C, which can be well adapted to industrial requirements.

The TEM images of fresh and used Pd@POPs are shown in Figure 2. No obvious big metal particles or clusters are observed in both of the TEM images, which suggests that the Pd active species are uniformly dispersed on the POP support. In addition, SEM mapping images of used Pd@POPs reveal that functional elements (P and Pd) are highly dispersed. It means that these elements are well integrated in the used Pd@POPs catalyst.

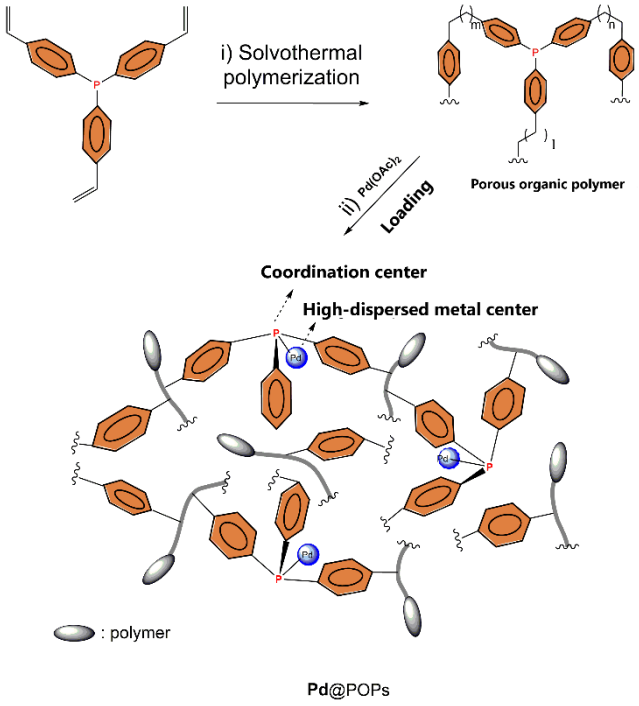

Scheme 1. Synthesis of the Pd@POPs catalyst.

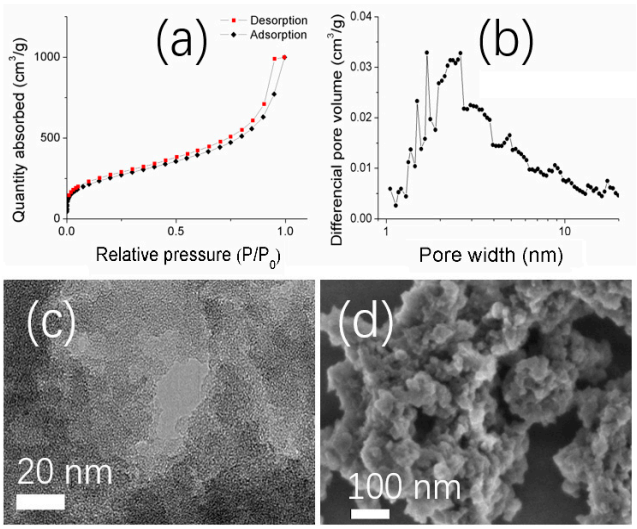

Figure 1. (**a**) N_2 adsorption–desorption isotherm of Pd@POPs, (**b**) pore size distribution of Pd@POPs, (**c**) TEM image of Pd@POPs, and (**d**) SEM image of Pd@POPs.

To explore the oxidation states of Pd species and the coordination effect between Pd and P, X-ray photoelectron spectroscopy (XPS) analysis was performed for POP and Pd@POPs, and the results are listed in Figure 3. The P2p spectrum (Figure 3a) mainly shows the presence of P with BE (Bonding Energy) = 131.79 and 130.42 eV in the POP backbone. After Pd loading, the binding energy of P2p (Figure 3b) shifts forward to a high field to 132.1 and 130.6 eV. In the Pd3d XPS spectrum (Figure 3c), four peaks with binding energies at 342.79 and 338.15 eV, which can be ascribed to Pd^{2+}, and 340.4 and 336.8 eV, which are assigned to Pd^0, can be deconvoluted. Compared with $Pd(OAc)_2$ (343.8 and 338.6 eV) [26], the Pd binding energy shifted negatively. These results demonstrate the coordination of Pd species with POP, in accordance with the conclusion of ^{31}P solid-state NMR. The presence of Pd^0 could be due to the fact that POP support possesses reducibility.

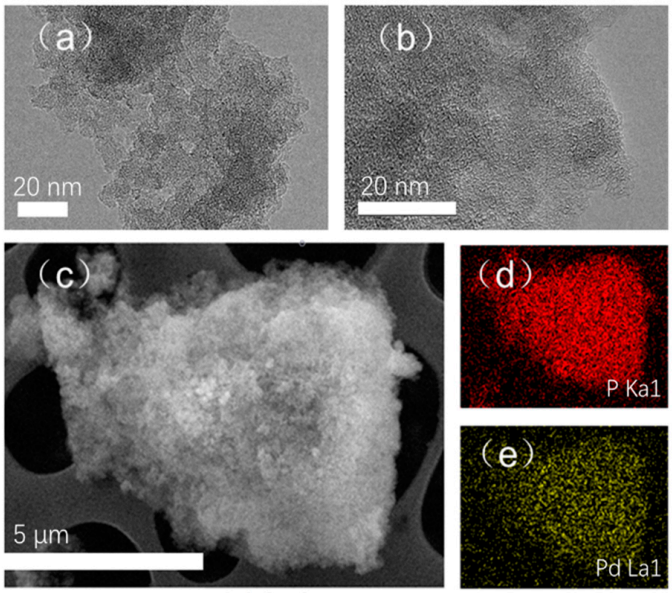

Figure 2. TEM images of (**a**) fresh and (**b**) used Pd@POPs, (**c**) SEM images of used Pd@POPs, SEM mapping images of used Pd@POPs, (**d**) P with red color, and (**e**) Pd with yellow color.

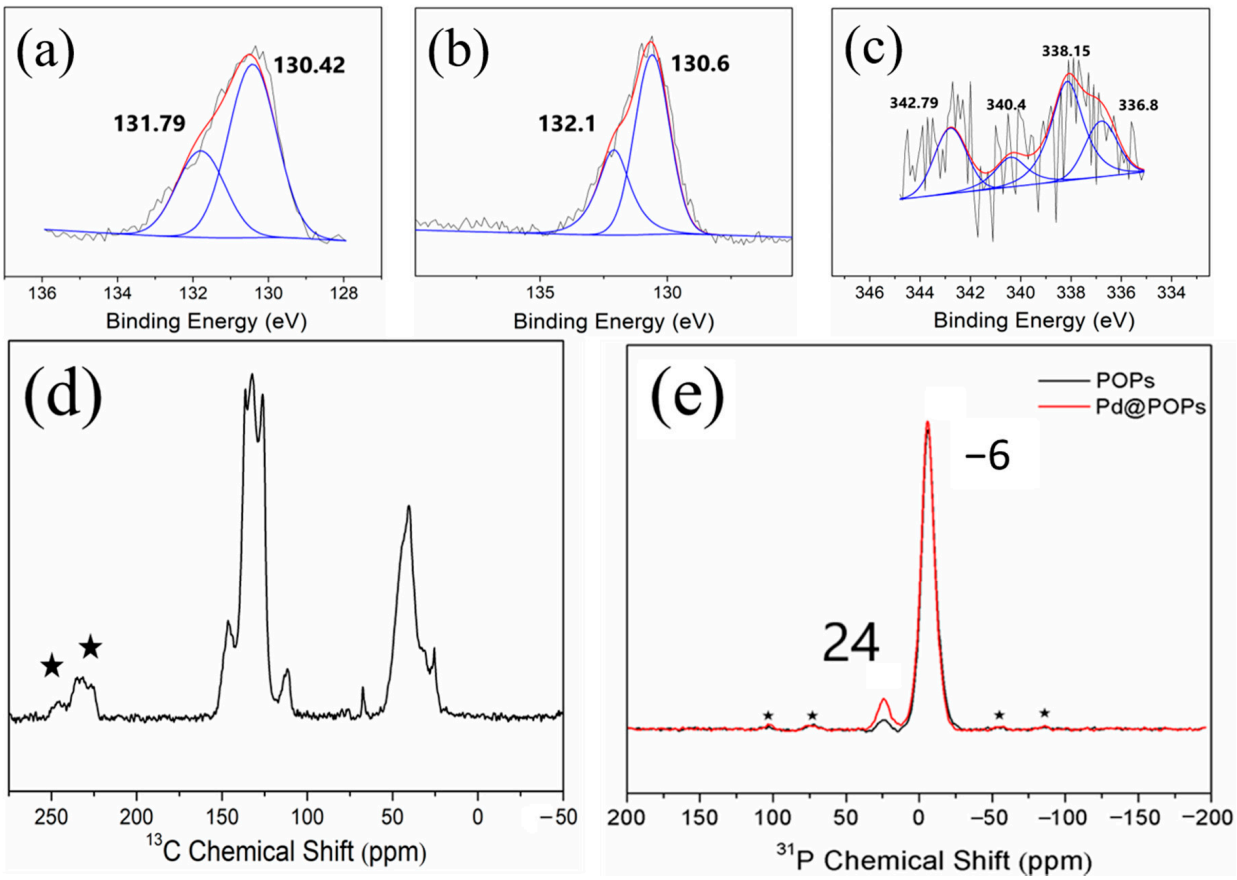

Figure 3. The XPS spectra of (**a**) P2p for POP and (**b**) P2p and (**c**) Pd3d for Pd@POPs. (**d**) The solid-state ^{13}C NMR spectrum of Pd@POPs. (**e**) The solid-state ^{31}P NMR spectrum of POP (black) and Pd@POPs (red). The peaks of spinning sidebands are marked with stars. For (**a**–**c**), the black lines are composed of original data, the red lines are fitting curves and the blue lines are got by peak fitting.

The solid-state ^{13}C NMR spectrum of Pd@POPs (Figure 3d) shows two strong broad peaks at 20–50 ppm (polymerized vinyl group) and 120–160 ppm (aromatic carbons), which suggests that the polymerization process was completed adequately. The solid-state ^{31}P NMR spectrum of Pd@POPs is employed to auxiliary XPS, proving the existence of a P–Pd coordination bond. The peak at −6 ppm in spectrum (Figure 3e) is assigned to the uncoordinated P specie. The peak at 24 ppm can be ascribed to the P specie coordinated with Pd due to the fact that the peak of 24 ppm is enhanced after Pd loading, which is consistent with the literature [27].

Sequentially, the catalytic activity of a few kinds of metal catalysts for the N-formylation reaction of morpholine to N-formylmorpholine was assessed, and the results are summarized in Table 1. The results show that the homogeneous catalyst of $Pd(OAc)_2$ gave a conversion of 49% (entry 1) in the absence of K_3PO_4. After adding K_3PO_4 to the reaction system, the conversion increased to 92% (entry 2). It means that alkali is beneficial to the formation of N-formylmorpholine, which is consistent with the literature [23,28]. Other precursors of Pd were researched, such as $PdCl_2$ (entry 3), showing a conversion of 71%. Some other metal catalysts were also investigated, and the results are listed in Table 1 (entry 4–6). $RhCl_3$ (entry 4) is almost not active for the N-formylation of morpholine with CO_2 in a homogeneous system, and the conversion is only 11%. Both $IrCl_3$ (entry 5) and $Co(NO_3)_2$ (entry 6) have low activity for N-formylation and get conversions of 36% and 20%, respectively. It can be concluded that the metal catalysts of palladium are more active for N-formylation than $RhCl_3$, $IrCl_3$, and $Co(NO_3)_2$. Therefore, we used $Pd(OAc)_2$ as the metal precursor to investigate the effect of supports.

Table 1. Catalytic performance of metal catalysts for N-formylation reaction.

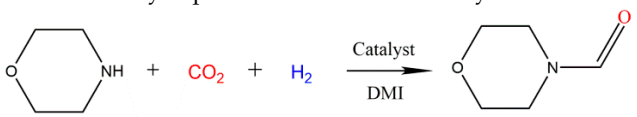

Entry	Catalyst	Conv.%
1 [a]	$Pd(OAc)_2$	49
2	$Pd(OAc)_2$	92
3	$PdCl_2$	71
4	$RhCl_3$	11
5	$IrCl_3$	36
6	$Co(NO_3)_2$	20

Conditions: morpholine, 1 mmol; precursor, 2.3 mol% based on morpholine; K_3PO_4, 0.3 mmol; $P_{CO2} = P_{H2} = 3$ MPa; DMI, 4 mL; 100 °C; 24 h; [a] no K_3PO_4.

A comparison of catalytic performances for Pd@supports is listed in Table 2, employing morpholine as a substrate. When POP was used as support (Pd@POPs), the catalyst obtained conversions of 92% (first run) and 91% (second run). By comparison, the conversions for the first run over Pd@SBA-15, Pd@Al_2O_3, and Pd@TiO_2 were 92%, 61%, and 93%, respectively, while the conversions for the second run of using Pd@SBA-15 and Pd@TiO_2 decreased to 82% and 71%, respectively. The decrease of catalytic activity may be attributed to the fact that the interaction between Pd and supports is not as strong as the coordination bond between Pd and P species in POP support. These results show that POP is more active and stable for the N-formylation of morpholine and CO_2 than catalysts with other supports we selected in the same reaction condition. The high BET surface areas, hierarchical pore structure, and Pd–P coordination bonds of the Pd@POPs catalyst are responsible for its improved catalytic performance. Compared with the Pd-based heterogeneous catalysts (Pd@NC, Pd/LDH) reported in the literature, Pd@POPs exhibits a similar activity under milder conditions.

Table 2. Comparison of the catalytic performance of Pd@supports.

Catalyst	CO_2/H_2/MPa	T/°C	Conv./%
Pd@POPs	3/3	100	92/91 [a]
Pd@SBA-15	3/3	100	92/82 [a]
$Pd@Al_2O_3$	3/3	100	61
$Pd@TiO_2$	3/3	100	93/71 [a]
Pd@NC [29]	3/4	130	93
Pd/LDH [30]	3/3	140	91.7

Conditions: morpholine, 1 mmol; Pd, 2.3 mol% based on morpholine (Pd loading is 0.5 wt%); K_3PO_4, 0.3 mmol; $P_{CO2} = P_{H2}$ = 3 MPa; DMI, 4 mL; 100 °C; 24 h. [a] The data were obtained with a reused catalyst for the second run.

Inspired by the above results, Pd@POPs was explored as a catalyst for the N-formylation of other secondary or primary amines (Table 3). The catalyst was successful for secondary amines, and the N-formylation products of cyclic secondary amines (1a-2a and 1b-2b) were synthesized with yields of 80–93% (entries 1–2). When aliphatic N-methylpentylamine was the substrate, a 61% yield of the corresponding formamide was obtained (entry 8). The Pd@POPs catalyst exhibited good applicability for secondary amines but was limited for primary amines. In Table 3, when primary amines, such as 4-methylbenzylamine (5a), were used as the raw material, the highest yield of 47% was achieved (entry 5). For other primary amines, including cyclohexamine (3a), benzylamine (4a), β-phenylethylamine (6a), 1-heptanamine (7a), and n-pentylamine (9a), the yields of the desired formamides were only 17–33% (entries 3, 4, 6, 7, 9).

Table 3. Substrate prolongation experiments of the Pd@POPs catalyst.

Entry	Substrate	Product	Conv.%
1	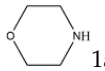 1a	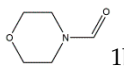 1b	93
2	 2a	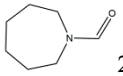 2b	80
3	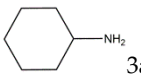 3a	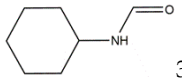 3b	17
4	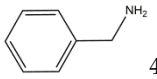 4a	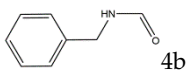 4b	22
5	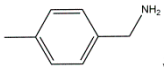 5a	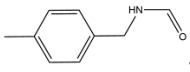 5b	47
6	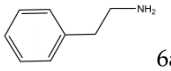 6a	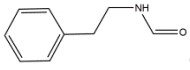 6b	33
7	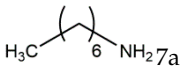 7a	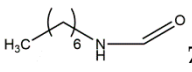 7b	30
8	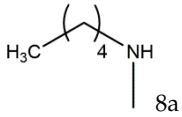 8a	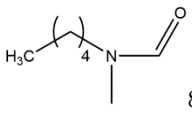 8b	61
9	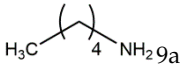 9a	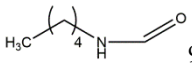 9b	24

Conditions: morpholine, 1 mmol; Pd, 2.3 mol% based on morpholine (Pd loading is 2.5 wt%); K_3PO_4, 0.33 mmol; $P_{CO2} = PH_2$ = 3 MPa; DMI, 4 mL; 100 °C; 24 h.

Additionally, the reusability of the Pd@POPs catalyst was studied. The results (Figure 4) suggest that the catalyst could be recycled at least five times without obvious loss of catalytic activity. The good stability is attributed to high P ligand concentrations, high surface areas, and stable coordination bonds between Pd species and P atoms in the POP support.

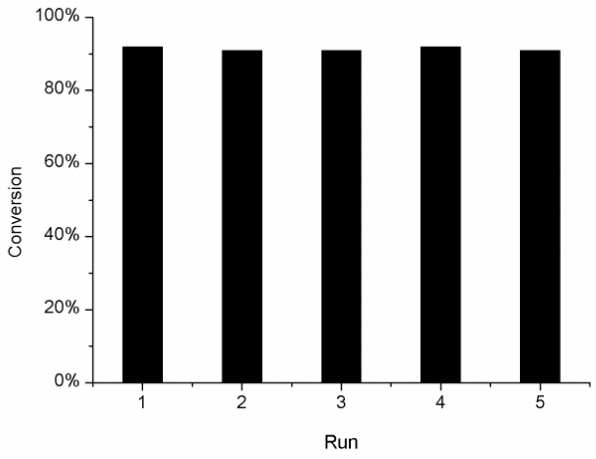

Figure 4. Recyclability tests of the Pd@POPs catalyst. Reaction conditions: morpholine, 1 mmol; catalyst Pd, 2.3 mol% based on morpholine (Pd loading is 0.5 wt%); K_3PO_4, 0.33 mmol; DMI, 4 mL; $P_{CO2} = P_{H2} = 3$ MPa; T = 373 K; t = 24 h.

As we know that the N-formylation reaction mechanism (Figure 5) is similar in most literatures, CO_2 is reduced to formic acid in a hydrogen atmosphere, and then reacts with amine to form amides [17,29,31]. We also demonstrated the reaction mechanism in a previous work [32].

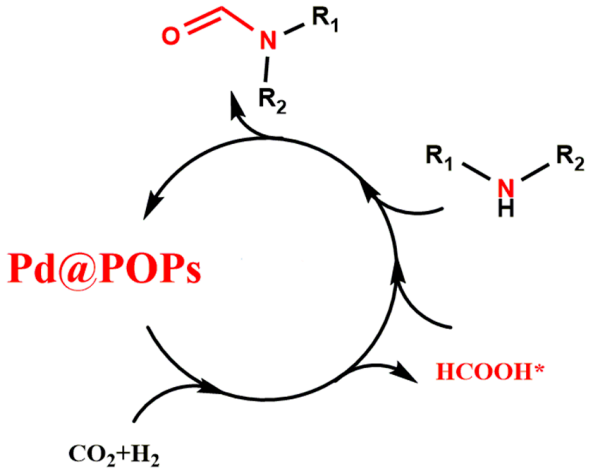

Figure 5. The possible mechanism of the N-formylation reaction.

3. Conclusions

In summary, we successfully synthesized a Pd@POPs catalyst by the solvothermal synthetic method for the N-formylation reaction of amine and CO_2. The Pd@POPs catalyst can immobilize Pd active species, which simplifies the recovery and reuse for the N-formylation reaction system. Especially, the heterogeneous catalyst has a good practical prospect because it not only is easy to synthesize but also has high catalytic efficiency and excellent stability. Characterization results indicate that the Pd@POPs catalyst has high BET surface areas, hierarchical pore structure, and uniform dispersion of Pd active species due to the formation of strong Pd–P coordination bonds. With the above-mentioned advantages, this method may be expected to replace the current ways for N-formylation reaction.

4. Materials and Methods

4.1. Material

All solvents and other chemicals were commercially available. Anhydrous THF (Tetrahydrofuran) is prepared by distillation from sodium benzophenone ketyl. The DMI ($\geq$99.5%) was purchased from the Macklin Biochemical Co., Ltd. (Shanghai, China).

4.2. Synthesis of PPh_3-POP

PPh_3-POP was synthesized by solvothermal polymerization. Typically, 100 mL THF was added into a 250 mL round-bottom flask loaded with a mixture of 3v-PPh_3 (tris-(4-vinylphenyl)-phosphine, 10 g), AIBN (2,2′-azobis(isobutyronitrile), 0.25 g), and a magnetic rotor. After stirring for 1 h to make it completely dispersed, the solution was transferred into an autoclave under Ar atmosphere. After sealing, the solution was kept at 100 °C for 24 h. After the system was cooled to room temperature, the polymer was collected by vacuum filtration and washed by THF. Then, the polymer was dried at 60 °C under vacuum for 12 h. Eventually, white powder was got and labeled as PPh_3-POP.

4.3. Synthesis of Pd@POPs

$Pd(OAc)_2$ (0.0108 g) was dispersed in 50 mL THF under Ar atmosphere. Afterwards, POP (1.0103 g) was introduced. The resulting mixture was stirred at room temperature for 24 h. The precipitate was collected by filtration and washed with THF. After drying at 60 °C under vacuum for 12 h, a pale-yellow powder was acquired and labeled as Pd@POPs.

4.4. Synthesis of Pd@SBA-15, Pd@Al_2O_3, and Pd@TiO_2

The Pd@SBA-15, Pd@Al_2O_3, and Pd@TiO_2 catalysts were prepared by the same method as described above except that POP was replaced with SBA-15, Al_2O_3, and TiO_2.

4.5. A Typical Procedure for N-Formylation Reaction

Pd@POPs (Pd loading was 2.3 mol% based on morpholine), morpholine (1 mmol), K_3PO_4 (0.3 mmol, 0.063 g), and DMI (1,3-dimethyl-2-imidazolidinone, 4 mL) were successively added into a stainless steel autoclave reactor (30 mL inner volume). The autoclave was purged by mixed gas three times and charged with the mixed gas (CO_2:H_2 = 1:1) up to 6 MPa at room temperature. Then the system was heated by an electric heating jacket to 100 °C and stirred for 24 h. The products were analyzed by Agilent 7890A (Santa Clara, CA, USA) gas chromatography (GC) with a capillary column (HP-5, 30 m × 0.32 μm diameter) using a flame ionization detector. Gas chromatography analysis used toluene as an internal standard. ^{1}H NMR spectra were acquired on Bruker AVANCE III NMR spectrometer (Kloten, Zürich, Switzerland) at 400 MHz using trimethylsilane (TMS) as an internal standard.

4.6. Recycling Stability of Pd@POPs Catalyst

The used catalyst was obtained by centrifugation after every cycle. The above catalyst was thoroughly washed with ethanol and THF. After drying at 60 °C under vacuum for 12 h, the used catalyst was reused for the next reaction cycle.

Supplementary Materials: The following are available online at https://www.mdpi.com/2073-4344/11/2/220/s1. Information on the characterization instruments, thermal gravimetric analysis (TGA, Figure S1), and GC or NMR spectra of the products (Figures S2–S10) can be obtained from Supplementary Materials.

Author Contributions: G.W. and M.J. have contributed evenly. Conceptualization—G.W., M.J., L.Y. and Y.D.; Formal analysis—G.J., Z.S., L.M. and H.D.; Investigation—G.W., M.J., G.J. and Z.S.; Methodology—C.L. and H.D.; Project administration—L.Y. and Y.D.; Writing–original draft—G.W.; Writing–review & editing—M.J., L.M., C.L., L.Y. and Y.D. The manuscript was written through contributions from all authors. All authors have read and agreed to the published version of the manuscript.

Funding: This work was funded by the National Natural Science Foundation of China (Grant No. 91845101), "Transformational Technologies for Clean Energy and Demonstration," Strategic Priority Research Program of the Chinese Academy of Sciences (Grant Nos. XDA 21020900 and XDB 17000000), DICP & QIBEBT (Grant No. DICP & QIBEBT UN201704), and Natural Science Foundation of Liaoning Province (Grant No. 2019-MS-324).

Data Availability Statement: The data presented in this study are available on request from the corresponding author.

Conflicts of Interest: The authors declare no conflict of interest.

References

1. Li, K.; Peng, B.; Peng, T.Y. Recent Advances in Heterogeneous Photocatalytic CO_2 Conversion to Solar Fuels. *ACS Catal.* **2016**, *6*, 7485–7527. [CrossRef]
2. Salehizadeh, H.; Yan, N.; Farnood, R. Recent advances in microbial CO_2 fixation and conversion to value-added products. *Chem. Eng. J.* **2020**, *390*, 124584. [CrossRef]
3. Haszeldine, R.S. Carbon Capture and Storage: How Green Can Black Be? *Science* **2009**, *325*, 1647–1652. [CrossRef]
4. Aresta, M.; Dibenedetto, A.; Angelini, A. Catalysis for the Valorization of Exhaust Carbon: From CO_2 to Chemicals, Materials, and Fuels. Technological Use of CO_2. *Chem. Rev.* **2014**, *114*, 1709–1742. [CrossRef] [PubMed]
5. Yu, K.M.K.; Curcic, I.; Gabriel, J.; Tsang, S.C.E. Recent Advances in CO_2 Capture and Utilization. *ChemSusChem* **2008**, *1*, 893–899. [CrossRef] [PubMed]
6. Vidal, J.L.; Andrea, V.P.; MacQuarrie, S.L.; Kerton, F.M. Oxidized Biochar as a Simple, Renewable Catalyst for the Production of Cyclic Carbonates from Carbon Dioxide and Epoxides. *ChemCatChem* **2019**, *11*, 4089–4095. [CrossRef]
7. Xiong, J.; Yang, R.X.; Xie, Y.; Huang, N.Y.; Zou, K.; Deng, W.Q. Formation of Cyclic Carbonates from CO_2 and Epoxides Catalyzed by a Cobalt-Coordinated Conjugated Microporous Polymer. *ChemCatChem* **2017**, *9*, 2584–2587. [CrossRef]
8. Wang, W.L.; Li, C.Y.; Yan, L.; Wang, Y.Q.; Jiang, M.; Ding, Y.J. Ionic Liquid/Zn-PPh_3 Integrated Porous Organic Polymers Featuring Multifunctional Sites: Highly Active Heterogeneous Catalyst for Cooperative Conversion of CO_2 to Cyclic Carbonates. *ACS Catal.* **2016**, *6*, 6091–6100. [CrossRef]
9. Yang, Z.Z.; Chen, H.; Li, B.; Guo, W.; Jie, K.C.; Sun, Y.F.; Jiang, D.E.; Popovs, I.; Dai, S. Topotactic Synthesis of Phosphabenzene-Functionalized Porous Organic Polymers: Efficient Ligands in CO_2 Conversion. *Angew. Chem. Int. Ed.* **2019**, *58*, 13763–13767. [CrossRef]
10. Chen, B.C.; Bednarz, M.S.; Zhao, R.L.; Sundeen, J.E.; Chen, P.; Shen, Z.Q.; Skoumbourdis, A.P.; Barrish, J.C. A new facile method for the synthesis of 1-arylimidazole-5-carboxylates. *Tetrahedron Lett.* **2000**, *41*, 5453–5456. [CrossRef]
11. Tohnishi, M.; Nakao, H.; Furuya, T.; Seo, A.; Kodama, H.; Tsubata, K.; Fujioka, S.; Kodama, H.; Hirooka, T.; Nishimatsu, T. Flubendiamide, a novel insecticide highly active against lepidopterous insect pests. *J. Pestic. Sci.* **2005**, *30*, 354–360. [CrossRef]
12. Gerack, C.J.; McElwee-White, L. Formylation of amines. *Molecules* **2014**, *19*, 7689–7713. [CrossRef] [PubMed]
13. Hauduc, C.; Belanger, G. General Approach toward Aspidospermatan-Type Alkaloids Using One-Pot Vilsmeier-Haack Cyclization and Azomethine Ylide Cycloaddition. *J. Org. Chem.* **2017**, *82*, 4703–4712. [CrossRef] [PubMed]
14. Huang, W.X.; Zhang, Z.H. Manufacturing Method of Novel Liquid PUR (Poly Urethane Resin) Cleaner. CN Patent CN109135961-A, 2017.
15. Zhang, L.; Han, Z.B.; Zhao, X.Y.; Wang, Z.; Ding, K.L. Highly Efficient Ruthenium-Catalyzed N-Formylation of Amines with H_2 and CO_2. *Angew. Chem. Int. Ed. Engl.* **2015**, *54*, 6186–6189. [CrossRef]
16. Daw, P.; Chakraborty, S.; Leitus, G.; Diskin-Posner, Y.; Ben David, Y.; Milstein, D. Selective N-Formylation of Amines with H_2 and CO_2 Catalyzed by Cobalt Pincer Complexes. *ACS Catal.* **2017**, *7*, 2500–2504. [CrossRef]
17. Dai, X.C.; Wang, B.; Wang, A.Q.; Shi, F. Amine formylation with CO_2 and H_2 catalyzed by heterogeneous Pd/PAL catalyst. *Chin. J. Catal.* **2019**, *40*, 1141–1146. [CrossRef]
18. Mitsudome, T.; Urayama, T.; Fujita, S.; Maeno, Z.; Mizugaki, T.; Jitsukawa, K.; Kaneda, K. A Titanium Dioxide Supported Gold Nanoparticle Catalyst for the Selective N-Formylation of Functionalized Amines with Carbon Dioxide and Hydrogen. *ChemCatChem* **2017**, *9*, 3632–3636. [CrossRef]
19. Ju, P.P.; Chen, J.Z.; Chen, A.B.; Chen, L.M.; Yu, Y.F. N-Formylation of Amines with CO_2 and H_2 Using Pd–Au Bimetallic Catalysts Supported on Polyaniline-Functionalized Carbon Nanotubes. *ACS Sustain. Chem. Eng.* **2017**, *5*, 2516–2528. [CrossRef]
20. Kaur, P.; Hupp, J.T.; Nguyen, S.T. Porous Organic Polymers in Catalysis: Opportunities and Challenges. *ACS Catal.* **2011**, *1*, 819–835. [CrossRef]
21. Yang, Z.Z.; Wang, H.; Ji, G.P.; Yu, X.X.; Yu, C.; Liu, X.W.; Wu, C.L.; Liu, Z.M. Pyridine-functionalized organic porous polymers: Applications in efficient CO_2 adsorption and conversion. *New. J. Chem.* **2017**, *41*, 2869–2872. [CrossRef]
22. Jiang, M.; Yan, L.; Ding, Y.J.; Sun, Q.; Liu, J.; Zhu, H.J.; Lin, R.H.; Xiao, F.S.; Jiang, Z.; Liu, J.Y. UltrasTable 3V-PPh_3 polymers supported single Rh sites for fixed-bed hydroformylation of olefins. *J. Mol. Catal. A Chem.* **2015**, *404*, 211–217. [CrossRef]
23. Li, C.Y.; Yan, L.; Lu, L.L.; Xiong, K.; Wang, W.L.; Jiang, M.; Liu, J.; Song, X.G.; Zhan, Z.P.; Jiang, Z.; et al. Single atom dispersed Rh-biphephos&PPh_3@porous organic copolymers: Highly efficient catalysts for continuous fixed-bed hydroformylation of propene. *Green Chem.* **2016**, *18*, 2995–3005.
24. Wang, Y.Q.; Yan, L.; Li, C.Y.; Jiang, M.; Zhao, Z.A.; Hou, G.J.; Ding, Y.J. Heterogeneous Rh/CPOL-BP&P$(OPh)_3$ catalysts for hydroformylation of 1-butene: The formation and evolution of the active species. *J. Catal.* **2018**, *368*, 197–206.
25. Wang, W.L.; Wang, Y.Q.; Li, C.Y.; Yan, L.; Jiang, M.; Ding, Y.J. State-of-the-Art Multifunctional Heterogeneous POP Catalyst for Cooperative Transformation of CO_2 to Cyclic Carbonates. *ACS Sustain. Chem. Eng.* **2017**, *5*, 4523–4528. [CrossRef]
26. Li, W.H.; Li, C.Y.; Li, Y.; Tang, H.T.; Wang, H.S.; Pan, Y.M.; Ding, Y.J. Palladium-metalated porous organic polymers as recyclable catalysts for chemoselective decarbonylation of aldehydes. *Chem. Commun.* **2018**, *54*, 8446–8449. [CrossRef] [PubMed]

27. Chen, X.K.; Wang, W.L.; Zhu, H.J.; Yang, W.S.; Ding, Y.J. Pd^0-$PyPPh_2$ @porous organic polymer: Efficient heterogeneous nanoparticle catalyst for dehydrogenation of 3-methyl-2-cyclohexen-1-one without extra oxidants and hydrogen acceptors. *Mol. Catal.* **2018**, *456*, 49–56. [CrossRef]
28. Kim, Y.J.; Lee, J.W.; Lee, H.J.; Zhang, S.Y.; Lee, J.S.; Cheong, M.; Kim, H.S. K_3PO_4-catalyzed carbonylation of amines to formamides. *Appl. Catal. A Gen.* **2015**, *506*, 126–133. [CrossRef]
29. Luo, X.Y.; Zhang, H.Y.; Ke, Z.G.; Wu, C.L.; Guo, S.E.; Wu, Y.Y.; Yu, B.; Liu, Z.M. N-doped carbon supported Pd catalysts for N-formylation of amines with CO_2/H_2. *Sci. China Chem.* **2018**, *61*, 725–731. [CrossRef]
30. Wang, Y.Y.; Chen, B.F.; Liu, S.L.; Shen, X.J.; Li, S.P.; Yang, Y.D.; Liu, H.Z.; Han, B.X. Methanol Promoted Palladium-Catalyzed Amine Formylation with CO_2 and H_2 by the Formation of $HCOOCH_3$. *ChemCatChem* **2018**, *10*, 5124–5127. [CrossRef]
31. Yu, X.X.; Yang, Z.Z.; Guo, S.E.; Liu, Z.H.; Zhang, H.Y.; Yu, B.; Zhao, Y.F.; Liu, Z.M. Mesoporous imine-based organic polymer: Catalyst-free synthesis in water and application in CO_2 conversion. *Chem. Commun.* **2018**, *54*, 7633–7636. [CrossRef]
32. Wang, G.Q.; Jiang, M.; Ji, G.J.; Sun, Z.; Li, C.Y.; Yan, L.; Ding, Y.J. Bifunctional Heterogeneous Ru/POP Catalyst Embedded with Alkali for the N-Formylation of Amine and CO_2. *ACS Sustain. Chem. Eng.* **2020**, *8*, 5576–5583. [CrossRef]